Colloids and Surfaces B: Biointerfaces 185 (2020) 110611

Contents lists available at ScienceDirect

Colloids and Surfaces B: Biointerfaces

journal homepage: www.elsevier.com/locate/colsurfb

Assessing the viability of Soluplus® self-assembled nanocolloids for sustained delivery of highly hydrophobic lapatinib (anticancer agent): Optimisation and *in-vitro* characterisation

Gunjan Vasant Bonde[a,b], Gufran Ajmal[a], Sarita Kumari Yadav[a,c], Pooja Mittal[a], Juhi Singh[a,d], Bharati V. Bakde[e], Brahmeshwar Mishra[a,*]

[a] Department of Pharmaceutical Engineering & Technology, Indian Institute of Technology, Banaras Hindu University, Varanasi, Uttar Pradesh, India
[b] School of Health Sciences, University of Petroleum and Energy Studies, Bidholi, Dehradun, Uttarakhamd, India
[c] Department of Pharmacy, Moti Lal Nehru Medical College, Allahabad, Uttar Pradesh, India
[d] Interdisciplinary Graduate Program, Nanyang Technological University, Singapore
[e] Pataldhamal Wadhwani College of Pharmacy, Yavatmal, Maharashtra, India

ARTICLE INFO

Keywords:
Anti-cancer agent
Breast cancer
Dilution test
Nanocarrier
Passive targeting
Pluronic® F127
Polymeric micelles

ABSTRACT

Nanocolloids are considered ideal carriers for hydrophobic drugs owing to their core–shell structure. Lapatinib is a potential anti-cancer agent, but its clinical use is limited because of its poor aqueous solubility, thus requiring larger oral doses with the associated toxicity. Thus, in the present study, we fabricated self-assembled nanocolloidal polymeric micelles (LP-PMs) of Soluplus® and Pluronic® F127 by the thin-film hydration method and assessed their delivery potential of the hydrophobic anti-cancer drug lapatinib (LP) and optimised these nanocolloidal polymeric micelles using Quality-by-Design approach. Amorphisation of the drug and no typical incompatibility other than hydrogen bonding in the LP-PMs was confirmed by solid-state characterisation. The LP-PMs exhibited a uniform size of 92.9 ± 4.07 nm, with a 5.06 mV zeta potential and approximately 87% drug encapsulation. The critical micellar concentration (CMC) of Soluplus® decreased from 6.63×10^{-3} to 4.4×10^{-3} mg/mL by incorporating Pluronic® F127. Further, the sustained release of LP from the LP-PMs was confirmed by *in-vitro* release studies showing 36% and 60% of LP released from the LP-PMs within 48 h in release media of pH 7.4 and pH 5.0, respectively. These results support their capability of preferential release at acidic tumor environment. Their hemocompatibility evidenced by hemolysis below accepted limits and no platelet aggregation with resistance to instant dilution illustrated their admirable blood compatibility and suitability for intravenous administration. The encapsulation of LP inside micelles enhanced the cytotoxicity of LP against SKBr3 breast cancer cells. Further, the LP-PMs were found to be stable over six months when stored at 2–8 °C. These findings indicate the improved potential of nanocolloidal polymeric micelles as promising carriers for the preferential and sustained delivery of hydrophobic anticancer drugs such as lapatinib to tumours.

1. Introduction

The design and development of nanocarrier systems for highly hydrophobic anti-cancer drugs is a challenging research area. However, in recent years, a few nanocarrier systems viz., nanoparticles, nanocapsules, nanocolloids, polymeric micelles (PMs), liposomes, polymeric microstructures, etc., have been investigated as sustained and targeted delivery systems to tumours [1–3]. Because of their higher encapsulation efficiency and pharmacokinetic features, nanocolloidal carrier systems have received significant attention in the area of

Abbreviations: BC, breast cancer; CMC, critical micelle concentration; DLS, dynamic laser scattering; EPR, enhanced permeation and retention; HER, human epidermal growth factor Receptor; HRSEM, high resolution scanning electron microscopy; LP, lapatinib; LP, PMs-lapatinib loaded polymeric micelles; LS, lapatinib solution; PF127, Pluronic® F127; PMs, polymeric micelles; RES, reticuloendothelial system; RH, relative humidity; AFM, atomic force microscopy

* Corresponding author at: Department of Pharmaceutical Engineering & Technology, Indian Institute of Technology, Banaras Hindu University, Varanasi, 221005, Uttar Pradesh, India.

E-mail addresses: gunjanvbonde@gmail.com (G.V. Bonde), gufranjamal86@gmail.com (G. Ajmal), saritayadav26@gmail.com (S.K. Yadav), poojamittal2009@gmail.com (P. Mittal), juhi.singh.phe13@itbhu.ac.in (J. Singh), bakdebharati@rediffmail.com (B.V. Bakde), bmishrabhu@rediffmail.com (B. Mishra).

https://doi.org/10.1016/j.colsurfb.2019.110611
Received 27 May 2019; Received in revised form 12 October 2019; Accepted 23 October 2019
Available online 29 October 2019

pharmaceutical research [4]. Among them, PMs have been of great interest for hydrophobic drug delivery because of their ability to enhance the solubility and bioavailability of hydrophobic drugs by virtue of their nanosize, typical core–shell structure [5,6] and exemplary therapeutic potential for cancer management owing to their tumour-targeting ability via the enhanced permeability and retention (EPR) effect [7]. The unique core–shell structure of these micelles comprises a corona of hydrophilic polymeric chains that envelops an inner core comprising hydrophobic segments, isolating the core from the aqueous exterior. This peculiar property of PMs facilitates the encapsulation of hydrophobic drugs via the solubilisation effect while the hydrophilic shell forms hydrogen bonds with the aqueous surrounding and improves the stability of the formulation *in-vitro* [8].

Further, the outer hydrophilic shell aids PMs in bypassing the recognition and non-specific phagocytosis by a reticuloendothelial system (RES) and prolongs the blood circulation time [1]. Beyond solubilisation and stability, hemocompatibility and reduced toxicity are important determinants of its success for drug delivery [9,10]. In the present study, we attempted the delivery of lapatinib (LP) (logP 5.45), an anti-cancer drug used to treat breast cancer, by entrapping LP inside the hydrophobic core of PMs, thus enhancing the aqueous solubility of the drug. The average particle size of the micelle (< 200 nm) is also favourable for their accumulation in tumours by passive targeting via the EPR effect [11].

Breast cancer (BC) is the second leading cause of death in women and there are expected to be about 1.98 million cases by 2020 [12]. LP was approved in 2007 for the treatment of HER2-positive advanced and metastatic BC in combination with capecitabine the US Food and Drug Administration (USFDA). LP is better at inducing tumour cell apoptosis and drug resistance reversal than monoclonal antibodies [13]. Unfortunately, the drug has poor aqueous solubility (7 μg/mL), resulting in restricted dissolution in gastrointestinal (GIT) fluids, and low oral bioavailability following oral administration. Regarding the oral route, LP also fails as an injectable therapeutic because it is insoluble in the solvents most frequently used for injectables [14]. Therefore, LP (Tykerb®, GlaxoSmithKline) must be administered in large daily doses (1250 mg/day), which induces serious side effects such as nausea, rashes, severe diarrhoea and hepatotoxicity [1]. Therefore, routes of administration other than oral must be investigated or various nanocarrier strategies must be employed to enhance solubility, bioavailability, and tumour targeting at low doses of the drug. The promising benefits offered by a micellar nanocolloidal system for delivery of a hydrophobic anticancer drug could be employed to fulfill the clinical as well as pharmaceutical needs for successful LP delivery.

Micellar forms are a significant characteristic of amphiphilic surfactants and polymers. Research in the area of polymer synthesis has come up with some novel amphiphilic polymers, viz. various grades of Pluronic®, Soluplus®, Solutol®, etc., for the development of micellar preparations. Soluplus® is a novel triblock polymer composed of a polyvinyl caprolactam-polyvinyl acetate-polyethylene glycol (57% vinyl caprolactam/30% vinyl acetate/13% PEG6000) having an average molecular weight ranging from 90,000 to 140,000 g/mol [15]. It was designed and produced by BASF to prepare solid solutions of poorly water-soluble drugs by hot-melt extrusion technology. It is amphiphilic, and thus it can be employed as a surfactant for the solubilisation of poorly water-soluble drugs. Soluplus® self-assembles as nanocolloidal micelles instantly in an aqueous environment to reduce the free energy above the critical micellar concentration (CMC) [16]. Therefore, it has been reported to be a favourable carrier for nanodelivery systems, displaying improved bioavailability and dissolution profiles [17]. Recently, its use in the improvement of poorly water soluble drugs and for sustained release of the drugs has been reported by several research groups [18–20].

The present work thus aimed to formulate a nanocolloidal PM dispersion for the loading of LP, a poorly water-soluble BCS Class II drug. The thermodynamic stability of the nanocolloidal PM dispersion was determined in terms of the CMC of the polymer/s and their combination. The PMs were optimised by using a Quality-by-Design (QbD) approach through proper selection of dependent and independent factors. The optimised nanocolloidal lapatinib polymeric micelles (LP-PMs) were evaluated to determine whether the encapsulation of LP could enhance its loading to a physiologically significant level. We also sought to demonstrate the ability of the proposed nanocolloidal formulation to sustain the delivery of the LP cargo over the intended period and to determine its anti-cancer efficacy and hemocompatibility for the safety of the patients.

2. Materials and methods

2.1. Materials

Lapatinib was purchased from Xi'an Kerui Biotechnology Co. Ltd (Xi'an, China). Soluplus® and Pluronic® F127 (PF127) was kindly gifted by BASF India Limited (Navi Mumbai, India). Other solvents of HPLC grade and Ultrapure Milli Q water were used throughout the studies. SKBr3 cell line was procured from National Centre for Cell Science, Pune while culture media and other necessary entities purchased from Himedia, India.

2.2. Determination of critical micelle concentration (CMC)

The CMC of Soluplus® and its mixture with PF127 (1% of dry weight of Soluplus®) was estimated by the iodine hydrophobic probe method [21]. The detailed procedure is given in Supplementary (S1.1). The profile of absorption intensity versus the logarithm of Soluplus® concentration was plotted. The value corresponding to a sharp increase in absorbance intensity is considered the CMC of Soluplus®.

2.3. Experimental design

The experimental model employed the Box–Behnken design (BBD), having three factors, three levels, and three centre points. Once designed, both statistical and mathematical techniques were applied using the response surface methodology (RSM) to assess the effect of each parameter. The dependent and independent variables were selected on the basis of previous studies from the literature and preliminary trial experiments. The ratio of drug to Soluplus® (A), amount of methanol (B), and the amount of surfactant i.e., PF127 (C) were chosen as the three independent factors, and the selected dependent factors were particle size (PS) (Y_1), polydispersity index (PDI) (Y_2) and encapsulation efficiency (EE) (Y_3). Table 1 summarises the set constraints and independent variables with their coded levels (high, medium, and low). The assessment of the experimental design was performed by employing Design Expert (STAT-EASE, 7.0.0, Minneapolis, MN) software and the significance of the parameters was determined by applying analysis of variance (ANOVA).

Moreover, the influence of all the three chosen independent variables on responses was assessed by studying the quadratic equations on the basis of the best-suited model, which is illustrated as follows:

$$Y = X_0 + X_1A + X_2B + X_3C + X_4AB + X_5AC + X_6BC + X_7A^2 + X_8B^2 + X_9C^2$$

where, Y = response, X_0 = constant, X_1, X_2, and X_3 = linear coefficients, X_4, X_5, and X_6 = interaction coefficients, and X_7, X_8 and X_9 = quadratic coefficients. A suitable model was then selected from the statistical data for instance, regression coefficient (R^2), Fisher's (F) value, p-value, and the lack of fit value. Then, the optimised batch was chosen by minimising the particle size and PDI and maximising EE; this optimised batch was then used for all physicochemical and *in-vitro* characterisation. The reliability of the developed mathematical models was validated by comparing predicted and experimental responses

Table 1
Composition of lapatinib-loaded polymeric micelles (LP-PMs) as per Box-Behnken design.

Batch Code	LP:Soluplus® ratio (w/w)	Methanol (mL)	Pluronic® F127 (%)	Paticle Size (nm)[a]	PDI[a]	EE[a] (%)	DL[a] (%)
1	0	0	0	93.6 ± 3.1	0.099 ± 0.012	84.71 ± 5.73	9.97 ± 0.67
2	0	−1	+1	116.0 ± 2.6	0.292 ± 0.016	82.53 ± 4.75	7.50 ± 0.43
3	0	−1	−1	125.2 ± 2.0	0.304 ± 0.030	72.31 ± 6.72	12.05 ± 1.12
4	+1	+1	0	72.8 ± 4.9	0.235 ± 0.032	83.82 ± 3.18	8.60 ± 0.33
5	−1	+1	0	112.3 ± 2.0	0.267 ± 0.004	72.75 ± 9.36	10.03 ± 1.29
6	0	0	0	94.9 ± 1.5	0.122 ± 0.028	84.79 ± 4.95	9.97 ± 0.58
7	−1	0	+1	130.4 ± 1.8	0.261 ± 0.029	71.86 ± 10.31	7.37 ± 1.06
8	0	0	0	92.9 ± 4.1	0.093 ± 0.018	82.13 ± 4.69	10.76 ± 0.90
9	+1	0	−1	108.8 ± 2.3	0.255 ± 0.005	75.81 ± 2.47	10.46 ± 0.34
10	0	+1	+1	97.9 ± 2.9	0.207 ± 0.014	84.02 ± 5.55	7.64 ± 0.51
11	−1	0	−1	108.4 ± 2.1	0.307 ± 0.022	64.03 ± 12.06	13.48 ± 2.54
12	0	0	0	95.5 ± 1.2	0.100 ± 0.010	84.05 ± 6.52	9.89 ± 0.77
13	0	0	0	95.4 ± 1.7	0.097 ± 0.007	86.07 ± 5.39	10.13 ± 0.63
14	+1	0	+1	79.9 ± 1.8	0.226 ± 0.007	81.49 ± 4.38	6.65 ± 0.36
15	0	+1	−1	102.6 ± 7.4	0.285 ± 0.062	88.14 ± 3.87	14.69 ± 0.65
16	−1	−1	0	120.8 ± 2.3	0.288 ± 0.013	71.84 ± 6.93	9.91 ± 0.96
17	+1	−1	0	112.8 ± 2.4	0.265 ± 0.012	79.78 ± 5.98	8.18 ± 0.61

[a] All the results are mentioned as mean ± standard deviation, n = 3.

using percent (%) bias [22].

2.4. Preparation of polymeric micelles

The LP-loaded micelles were fabricated by a previously described thin-film hydration method with slight modifications [23]. Briefly, the defined amount of LP and Soluplus® were dissolved in the appropriate quantity of methanol in a beaker with constant stirring until a clear solution was obtained. The solution was then transferred to a round-bottom flask, and the methanol was evaporated to form a thin film by rotary evaporator at 35 °C and 60 rpm under vacuum. The film was then vacuum dried overnight to ensure complete removal of methanol. Next day, the film was hydrated by adding 10 mL of warm deionised water containing PF127 and rotating it at 80 rpm for a further 30 min to prepare a micellar dispersion. The dispersion was then filtered through a 0.45-µm filter to filter out aggregated and unincorporated drug.

2.5. Solid-state characterisation of LP-PMs

2.5.1. Fourier transform infra-red (FT-IR) study

The FT-IR spectra of LP, Soluplus®, PF127, physical mixtures of all excipients and the LP-PMs were recorded on FT-IR (SHIMADZU 8400S, Japan). (See S1.2) The spectra were scanned and recorded in the range of 4000 cm^{-1} to 400 cm^{-1} to investigate the polymer-drug interactions.

2.5.2. X-ray powder diffraction (XRPD) study

The XRPD patterns of LP, Soluplus®, PF127, physical mixtures of all excipients and the LP-PMs were recorded using Rigaku portable X-ray diffractometer (Rigaku, Japan), using nickel-filtered Cu Kα radiation generated (whereas the X-ray tube was operated at a potential at 40 kV and 25 mA). The diffractogram was scanned over a 2θ range of 5–70° with a scanning rate of 2°/min and step size 0.02°.

2.5.3. Particle size analysis

The average particle size, polydispersity index (PDI) and zeta potential of the PMs was determined by the principle of dynamic laser scanning (DLS) technique employed by Beckman Coulter Particle Analyzer (Delsa™Nano C). The instrument was equipped with a He-Ne laser. All the measurements were carried out at scattering angle fixed of 165°.

2.5.4. Morphological characterization

The particle size analysis and morphological observations were performed by employing High Resolution-Scanning Electron Microscopy (HR-SEM) (FEI-Nova NanoSEM 450), operated at 15 kV and Atomic Force Microscopy (AFM) (NT-MDT, NTGRA PRIMA, Russia) (See S1.3 for sample preparation method).

2.6. Encapsulation efficiency (EE) and drug loading (DL)

The EE and DL of the LP-PMs were measured using UV-spectrophotometer (Shimadzu UV-1800). In brief, a defined volume of the formulation was dissolved in methanol and further diluted up to 1 mL. The solution was sonicated and vortexed to dissolve the formulation and centrifuged at 15,000 rpm at 4 °C for 15 min. The collected supernatant was suitably diluted with methanol, and the absorbance was recorded at λ_{max} of 261.5 nm. Based on the standard curve of LP in methanol, the concentration of LP was calculated and the EE and DL were determined by using following equations:

$$\text{EE}\,(\%) = \frac{\text{Amount of LP entrapped in PMs}}{\text{Initial amount of LP}} \times 100$$

$$\text{DL}(\%) = \frac{\text{Amount of LP entrapped in PMs}}{\text{Total dry weight of LP}-\text{ PMs}} \times 100$$

2.7. In-vitro cumulative drug release studies

The reported dialysis bag method, from literature with necessary modifications, was employed to perform an *in-vitro* release study of the LP-PMs (for details see S1.4) [24]. The released LP was detected by UV-spectrophotometer. The cumulative percent drug release was also calculated.

2.8. Hemocompatibility study

The hemocompatibility study involved the collection of blood samples from volunteers in heparinised tubes. The blood samples were centrifuged for 10 min at 5000 rpm to isolate the erythrocytes from the plasma; the erythrocytes were then washed three times with physiological saline. The isolated erythrocytes (900 µL) were mixed with a series of dilutions of pure drug suspensions and LP-PMs. After gentle mixing, these were incubated for 1 h at room temperature. Physiological saline (4 mL) was added to the mixture, which was then centrifuged for 15 min at 10,000 rpm. The erythrocytes incubated with 0.5% Triton-X100/blood and physiological saline/blood served as a positive control (PC) and negative control (NC), respectively. The separated supernatant

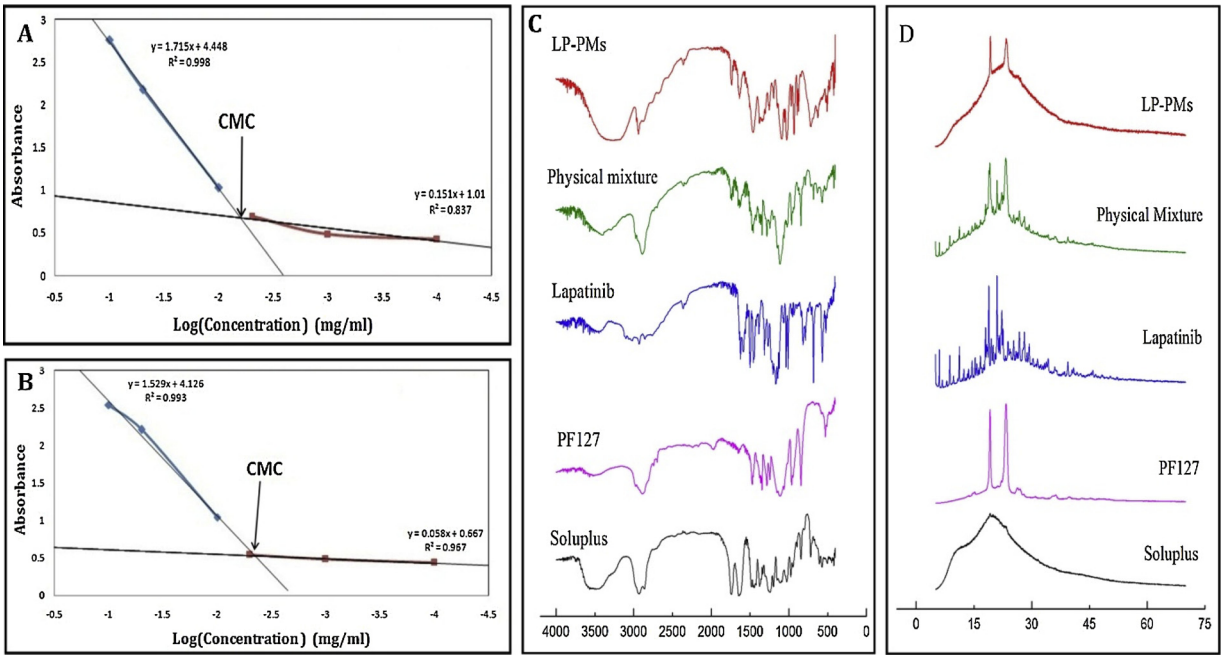

Fig. 1. Critical micelle concentration (CMC) determination of (A) Soluplus® and (B) mixture of Soluplus® and Pluronic® F127 (PF127); Solid state characterization: (C) FT-IR spectra and (D) X-ray diffractogram of Lapatinib-loaded polymeric micelles (LP-PMs) and pharmaceutical excipients.

was quantified by measuring its optical density (OD) at 540 nm with a UV-spectrophotometer. The following equation was used to estimate the percent (%) hemolysis [25]:

$$\text{Haemolysis}\ (\%) = \frac{OD_{test} - OD_{NC}}{OD_{PC} - OD_{NC}} \times 100$$

2.9. Platelet aggregation test

The reported method by Bender et al. was then used [26]. LP-PMs were incubated with citrated whole blood at 37 °C for 30 min with intermittent agitation; PBS pH 7.4 and collagen (2 µg/mL) served as the negative and positive control, respectively. Smears of treated blood were prepared on glass slides and air dried. Cells were stained with Leishman's stain (Span Diagnostic, India) and then rinsed with water. The air-dried slides were then observed by optical microscope (Dewinter Trinocular Microscopic Unit, Dewinter Technologies).

2.10. Effect of dilution on physical stability of LP-PMs

To assess the integrity of the LP-PMs when diluted to higher extents, simulating intravenous administration, the LP-PMs were diluted to 10, 100, 200, 400, and 500 times with de-ionised water, simulating aqueous body fluids. The particle size of the LP-PMs in diluted solutions was then measured, as given in 2.5.3.

2.11. Stability studies

Stability studies were conducted to verify the stability of the optimised LP-PMs in different environmental conditions. According to protocol, the LP-PMs were stored at 30 ± 2 °C/65 ± 5% relative humidity (RH) (for long term at room temperature) and 5 ± 3 °C (for refrigerated condition) for 6 months. The samples were withdrawn at 0, 3, and 6 months and evaluated in terms of change in particle size, PDI, and EE. The temperature conditions were selected according to Q1A (R2) ICH guidelines. Minitab® ver. 17 was used to estimate the shelf life [27].

2.12. In-vitro anti-cancer efficacy studies

The SKBr3 cancer cell line was cultured in McCoy's 5A medium (with 10% fetal bovine serum, 100 mg/mL streptomycin, 100 U/mL penicillin) and incubated at 37 °C and 5% CO_2. The cells (10^4 cells/well) were seeded in a 24-cell culture plate and treated with mix of Soluplus® and PF127, placebo micelle, LP solution (LS) and LP-PMs (10 µg of LP/mL) for 24 h. The cells were then carefully washed with PBS three times and fixed by 4% paraformaldehyde in PBS (pH 7.4) for 15 min at room temperature. Fixed cells were washed with PBS again and mounted on glass slides. The slides were then observed under inverted light microscope

2.13. Statistical analysis

All the results are articulated in the form of mean ± standard deviation (SD). Statistical comparisons were carried out by student (unpaired) *t*-test and one-way/two-way analysis of variance (ANOVA) by employing the GraphPad Prism (GraphPad Prism Software, USA). The disparity was supposed to be statistically significant when $p < 0.05$ (95% Confidence Interval).

3. Results

3.1. Determination of critical micelle concentration (CMC)

The iodine hydrophobic probe method employs iodine (I_2) as a hydrophobic probe whose absorbance abruptly increases as the amphiphiles get converted to micellar form and the corresponding polymer concentration is considered the CMC. The profile of absorption intensity versus Soluplus® concentration is illustrated in Fig. 1(A, B). The observed CMC of Soluplus® was 6.63×10^{-3} mg/mL, which is in good agreement with the previously reported value of 7.6×10^{-3}mg/mL [18,28], and higher than reported values of generally used surfactants such as Tween® 21 (2.84×10^{-3}mg/mL) [29]. However, the addition of another amphiphilic polymer, PF127, decreased the CMC value to 4.4×10^{-3}mg/mL.

3.2. Experimental design

In the present work, the BBD experimental design was employed, which consisted of 17 runs with three factors and three levels. The interaction of the independent variables and their effect on responses were analysed by Design Expert Software. On the basis of these interactions and the optimised levels of independent variables, an optimised formulation (LP-PMs) was prepared. The experimental findings for each response are recorded in Table 1.

3.2.1. Effect on particle size

The average PSs of the micelles ranged from 72.8 ± 4 nm to 130.4 ± 7 nm (Table 1). The negative coefficients of the chosen independent variables imply significant ($p < 0.05$) negative effects on PS; the relation is well understood by the following polynomial equation:

$$\text{Particle Size} = 94.84 - 11.99A - 11.27B - 2.21C - 7.43AB - 12.70AC + 1.93\,BC + 3.78A2 + 6.55B2 + 8.23C2$$

The Model F-value of 476.63 ($p < 0.05$) suggests the significance of the chosen model. The "Lack of Fit F-value" of 4.16 was insignificant. However, "Predicted R^2" of 0.9796 was in legitimate agreement with the "Adjusted R^2" of 0.9963, which indicates the adequacy of the model.

3.2.2. Effect on polydispersity index

The effect of the independent variables on PDI is illustrated in Fig. 2(C, D) and can be well understood by the following equation:

$$PDI = 0.10 - 0.018A - 0.019B - 0.021C - 2.250AB + 4.250AC - 0.016\,BC + 0.076A2 + 0.086B2 + 0.084C2$$

The average PDI of the micelles ranged from 0.093 ± 0.018 to 0.304 ± 0.030 (Table 1), and the selected independent variables had a significant effect ($p < 0.05$) on PDI. Further, the Model F-value of 79.61 ($p < 0.05$) suggests the significance of the chosen model. The "Lack of Fit F-value" of 1.30 was insignificant. The "Predicted R^2" of 0.9158 was in agreement with the "Adjusted R^2" of 0.9779, which indicates the adequacy of the model.

3.2.3. Effect on encapsulation efficiency

The average EE of the formulations was found to range from 64.03 ± 12.06%–88.14 ± 3.88% (Table 1). The effect of the independent variables on EE is given by the following equation:

$$EE = 93.52 + 5.05A + 2.78B + 2.45C + 0.78AB - 0.54AC - 3.59BC - 12.46A^2 - 4.01B2 - 7.76C2$$

The positive coefficients suggest a direct and significant ($p < 0.05$) relationship between the independent variables and EE. Similarly, the Model F-value of 28.55 ($p < 0.05$) suggests the significance of the chosen model, whereas the "Lack of Fit F-value" of 2.88 suggests its non-significance. From the three-dimensional (3D) response surface plots [Fig. 2(E, F)], it can be seen that by keeping one variable constant, the other two had optimum effects around the mid-points of the design.

By statistically analysing the above experimental findings, LP-PMs were optimised by Expert Design Software, keeping the variables, viz. PS and PDI, minimised while maximising EE. The LP-PMs contained a drug:polymer ratio of 1:5.46, 21.78 mL of methanol, and 0.59% PF127, with 0.887 desirability. The prepared LP-PMs were then used for subsequent evaluations and the results are given in Table 2.

3.3. Preparation of polymeric micelles

The conventional methods employed for preparing PMs include the direct dissolution method, dialysis method, film sonication method, thin-film hydration technique (solvent evaporation method), etc. The physicochemical characteristics of the excipients and drugs are the deciding factors for the selection of a suitable method of PM preparation. In the present work, we used the thin-film hydration method.

3.4. Solid-state characterization of LP-PMs

3.4.1. Fourier transform infra-red study

The Fourier transform infra-red (FT-IR) spectra of LP, Soluplus®, PF127, the physical mixture, and the LP-PMs are shown in Fig. 1(C). The spectra of LP consisted of characteristic absorption peaks at 785 cm^{-1} (C–Cl aromatic), 1147 cm^{-1} (C—F aromatic), 1313 cm^{-1} (O = S═O), 3065 cm^{-1} (N—H stretching), etc [30]. For Soluplus®, absorption bands appeared at 3350–3650 cm^{-1} (intermolecular hydrogen bonded O—H stretching), 1734 cm^{-1} [carbonyl stretching of $OC(O)CH_3$ of ester], and 1636 cm^{-1} [carbonyl stretching of C(O)N of amide] [31]. Moreover, the spectra of PF127 exhibited peaks at 1112 cm^{-1}, 1344 cm^{-1}, and 2883 cm^{-1}, which may be assigned to C—O stretching, in-plane O—H bending and C—H stretching of the aliphatic portion O, respectively [32].

3.4.2. X-ray powder diffraction study

The existing states of LP, PF127, Soluplus®, the physical mixture, and the LP-PMs were confirmed via XRPD analysis, and the recorded X-ray diffractogram are shown in Fig. 1(D). LP exhibited a crystalline nature as its diffractogram contained sharp characteristic peaks at 18.04°, 18.9°, and 21.02°; data resembled those reported in previous literature. The broad halo with no sharp peaks in the XRPD pattern of Soluplus® revealed its amorphous nature, whereas PF127 exhibited two sharp peaks at 19.22° and 23.36°. The XRPD pattern of the physical mixture displayed a mere superimposition of the above three diffractograms with attenuated intensity to some extent, suggesting the presence of crystalline LP and PF127 in the physical mixture. However, the LP-PMs exhibited a broad halo corresponding to Soluplus® with two superimposed peaks (19.32° and 23.4°) corresponding to PF127 without any typical reflection peaks of LP.

3.4.3. Particle size analysis

The LP-PMs were well dispersed in aqueous medium. The hydrodynamic diameter and PDI were analysed by DLS technique, and the results are presented in Table 2. It can be seen from Fig. 3(A) that diameters of the optimised LP-PMs were 92.9 ± 4.07 nm (8.04% bias) with a PDI of 0.093 ± 0.083.These results are in good agreement with the values predicted by the quadratic model. The lower PDI confirmed the successful preparation of monodispersed and uniform-sized micelles. Further, the sizes of the micelles increased from 57.2 nm for blank micelles (without LP) to 95.2 nm for the LP-PMs [Fig. 3(A)].

The zeta potentials of the optimised LP-PMs and blank micelles were 5.06 mV and -4.84 mV, respectively, shown in Fig. 3(A).

3.4.4. Morphological characterization

The evaluation of the morphology using high-resolution scanning electron microscopy (HR-SEM) [Fig. 3(B)] revealed the spherical shape of the micelles. The sizes of the micelles varied between 62–95 nm, with an average diameter of 81.85 ± 12.44 nm, which was slightly smaller than the results of the DLS studies.

The surface roughness of the micelle films was verified by AFM, and it was found that the micelles were spherical Fig. 3(B), with an average peak-to-peak height of 65 nm, which may correspond to the apparent diameter of the micelles. These results were in good agreement with those of the HR-SEM studies.

3.5. Encapsulation efficiency and drug loading

The EE and DL of the LP-PMs were found to be 87.23 ± 4.85% (-7.428% bias from the predicted value) and 9.27 ± 0.52%, respectively.

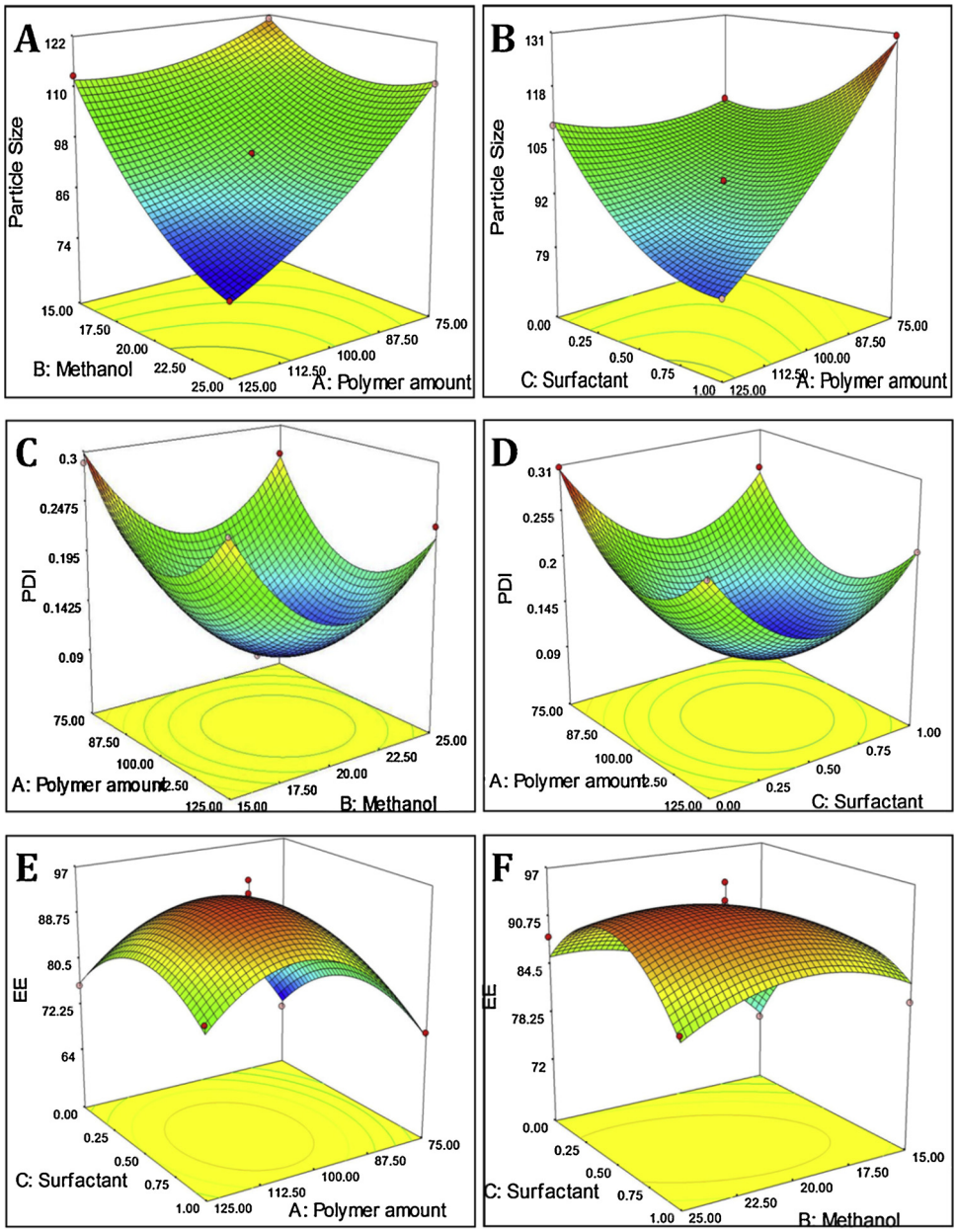

Fig. 2. 3-D response-surface plots showing: (A&B) Effect of independent factors on particle size; (C&D) Effect of independent factors on polydispersity index; and (E& F) Effect of independent factors on encapsulation efficiency.

3.6. In-vitro cumulative drug release studies

An *in-vitro* release study of the LP-PMs was performed using the dialysis bag method. Tween® 80 (0.5%) was added to the release media in order to maintain a sink condition. The released LP was detected by UV-spectrophotometer, as described above. The cumulative percent release was also calculated. The impact of pH on drug release is shown in Fig. 4(A). At the end of the first 24 h, nearly 29% of LP had been released at pH 7.4. However, drug release slowed and 36% of the drug was released over 48 h. At pH 5.0, the total LP release was found to be 45% and 60% at the end of 24 h and 48 h, respectively. The drug release data were integrated into different kinetic models, and it was found that the LP release followed the Higuchi model.The value of the Peppas exponent *n* was found to be 0.477, which suggests that the LP release followed Fick's diffusion.

3.7. Hemocompatibility study

In the present study, no significant hemolysis, i.e., below a limit of 1%, was found in either the LP-PMs or LP-only at the four different concentrations. However, significantly lower hemolysis ($p < 0.01$) was found in the LP—PMs group as compared to the LP-only group, as depicted in Fig. 4(B).

3.8. Platelet aggregation test

Fig. 4(C) shows that platelets with normal and discoid shapes were dispersed discretely all over the slide; no aggregation was observed in either the control or the LP-PM–treated blood samples.

3.9. Effect of dilution on physical stability of LP-PMs

The observed PSs gradually decreased from 126.47 ± 5.28 nm for

Table 2
Predicted and experimental values for optimised LP-PMs.

Independent variables			**Predicted Levels for optimization**
X_1 :	API:Polymer ratio (w/w)	–	1:5.46
X_2 :	Methanol (mL)	–	21.78
X_3 :	Co-surfactant (%)	–	0.59
Dependent variables			**Constraints for optimization**
Y_1 :	Particle size (nm)	–	Minimum
Y_2 :	Polydispersity index	–	Minimum
Y_3 :	Entrapment efficiency (%)	–	Maximum
Desirability of model: 0.887			
Response:		**Predicted values**	**Experimental values**[a]
Particle size (nm)		85.99 nm	92.9 ± 4.07 nm
Polydispersity index		0.108	0.093 ± 0.083
Entrapment efficiency (%)		94.226	87.23% ± 4.85 %

[a] All the results are mentioned as mean ± standard deviation, n = 3.

the original solution to 121.67 ± 9.07, 107.47 ± 7.25, and 93.03 ± 10.18, and 56.60 ± 7.69 nm upon dilution 10, 100, 200, and 400 times, respectively, with water. However, the solution was transparent beyond 500 times dilution, and no data could be recorded by DLS, which indicated the absence of micelles in the diluted bulk.

3.10. Stability studies

The LP-PMs were stored at two different temperature and relative humidity conditions to observe the effect of the environment on their stability. The changes observed in PS, PDI, and EE at each sampling time were non-significant ($p < 0.05$) when the LP-PMs were stored at 5 ± 3 °C. However, significant changes were observed within the first three months at the storage condition of 30 ± 2 °C/65 ± 5% RH, and hence these LP-PM batches were withdrawn from the study protocol. The results for each evaluation attribute before and after the sampling time are tabulated in Table 3. Further, the shelf life, estimated from the EE with the help of Minitab® version 7, was estimated to be 12 months, as shown in Fig. 5(A).

3.11. In-vitro anti-cancer efficacy studies

Fig. 5(B) shows morphological changes in SKBr3. Untreated SKBr3 cells exhibit natural cuboidal and polygonal shape with abundant cells in the field of vision (FOV). LP-PM-treated cells showed rounded and smaller cells (#), more granular cytoplasm ($), and a few cells with loss of confluence (*) in the FOV. Further, LS-treated cells exhibited their original morphology, but some of the cells showed altered and rounded morphology. Similarly, cells treated with mix of surfactants, placebo micelle and LS also retained their original morphology, but a few cells showed rounded morphology.

4. Discussion

The study was aimed at the preparation and evaluation of Soluplus® polymeric micelles of LP for their potential to serve as nanocarriers for highly hydrophobic anti-cancer drugs and their safety and efficacy by the I.V. route. Although LP is a potential anti-cancer drug, its clinical use is limited because it is currently available only in tablet form at larger doses with increased toxicity. Thus, we attempted to prepare LP-PMs as a micellar preparation intended for I.V. administration. In the present research, we particularly focused on the design and optimization of the nanocarrier system and the evaluation of the delivery and *in-vitro* performance of LP-PMs.

For the preparation of the micelle, amphiphilic polymers with low CMC values are needed. CMC is a crucial characteristic of amphiphilic polymers in determining the *in-vitro* and *in-vivo* kinetic stability (disassembly rate) and thermodynamic stability (disassembly potential), as well as the solubilisation capacity of PMs. The addition of PF127 reduced the CMC of Soluplus®. The reduction in CMC was credited to the increased contribution of hydrophobic portions of the polymers and their enhanced interaction with the aqueous surrounding [33]. The findings can be explained on the basis of two reported phenomena. First, surfactants were adsorbed onto the surfaces of the micelles to lower the surface tension. The intercalation of molecules from another surfactant with those of the first surfactant further reduced to surface tension. Therefore, a smaller amount of mixed surfactant was required to lower the surface tension below CMC, thereby achieving micellelisation at lower concentrations. Thus, the synergism of the two surfactants lowered the CMC of the mix [34]. Second, it has been reported by many researchers that the CMC is lowered when the chain length of the hydrophobic part or, in other words, the hydrophobic portion, increases [35]. The higher proportion of hydrophobic part favours the feasible micellar form to achieve thermodynamic stability by reducing the interaction of the increased hydrophobic portions with the aqueous portion, reducing the CMC [34,36]. Thus, thermodynamic stability is inversely proportional to the CMC and directly proportional to the length of the hydrophobic chain/portion and the contribution of the hydrophobic portion of the amphiphile [35,37]. Similar synergistic effects for lowering the CMC for surfactants mixture were previously reported by Rehman et al. for mixture of Tween 80 and Tween 20 [38], by Nagarajan for mixture of polymer and surfactant [39] and by Bhuptani et al. for Soluplus® and Solutol® HS 15 [40].

Further, the stability of the LP-PMs was also confirmed by diluting the LP-PMs with deionised water. We found that with up to 400-fold dilution of the LP-PMs, the micellar form was maintained; however, the micelle size continued to decrease with increasing dilution. Upon further dilution (500 times), the amphiphile concentration fell well below the CMC value, which consequently induced the dissociation of the micellar system completely. The observed reduction in the size with increasing dilution can be justified by the well-known fact that component amphiphilic polymer molecules are always in dynamic equilibrium with the free molecules in the bulk of dispersion. The concentration of amphiphiles decreased gradually during the serial dilution, and the concentration of the amphiphiles in bulk may be maintained by a reduction in the number of amphiphiles who took part in the micelle formation before dilution, which may be the reason for the reduction of PS upon dilution. Similar facts were also previously reported in the literature [21,41]. On the basis of findings of CMC determination and dilution effect studies, the very low CMC values of Soluplus® and its combination with PF127 suggests the higher thermodynamic and kinetic stability of prepared LP-PMs, which ensures the unhampered integrity and less sensitivity of the LP-PMs towards dilution in large amounts of the biological fluids, avoiding burst release during post-oral/intravenous administration [42].

The concept of design of experiment (DoE) trials makes it possible to understand the relation between dependent and independent variables, as well as the individual and interactive effects of these variables on the output responses by designing the experiments in an organised manner. We optimised the LP-PM formulations according to the BBD design, and 3D surface plots are illustrated in Fig. 2. From Fig. 2(A, B), it was concluded that the mean PS decreased remarkably with increasing methanol, which may have been due to the formation of a more uniform film during drying and the film formation phase. However, the surfactant had an optimum effect around the midpoint, which can be better understood by the fact that the surfactants reduced the surface tension to reduce PS, but a further increase in PS beyond the mid-point may have been due to the incorporation and aggregation of excess surfactant molecules over the surface of the already prepared micelles.

Further, with increases in the amount of methanol and surfactant,

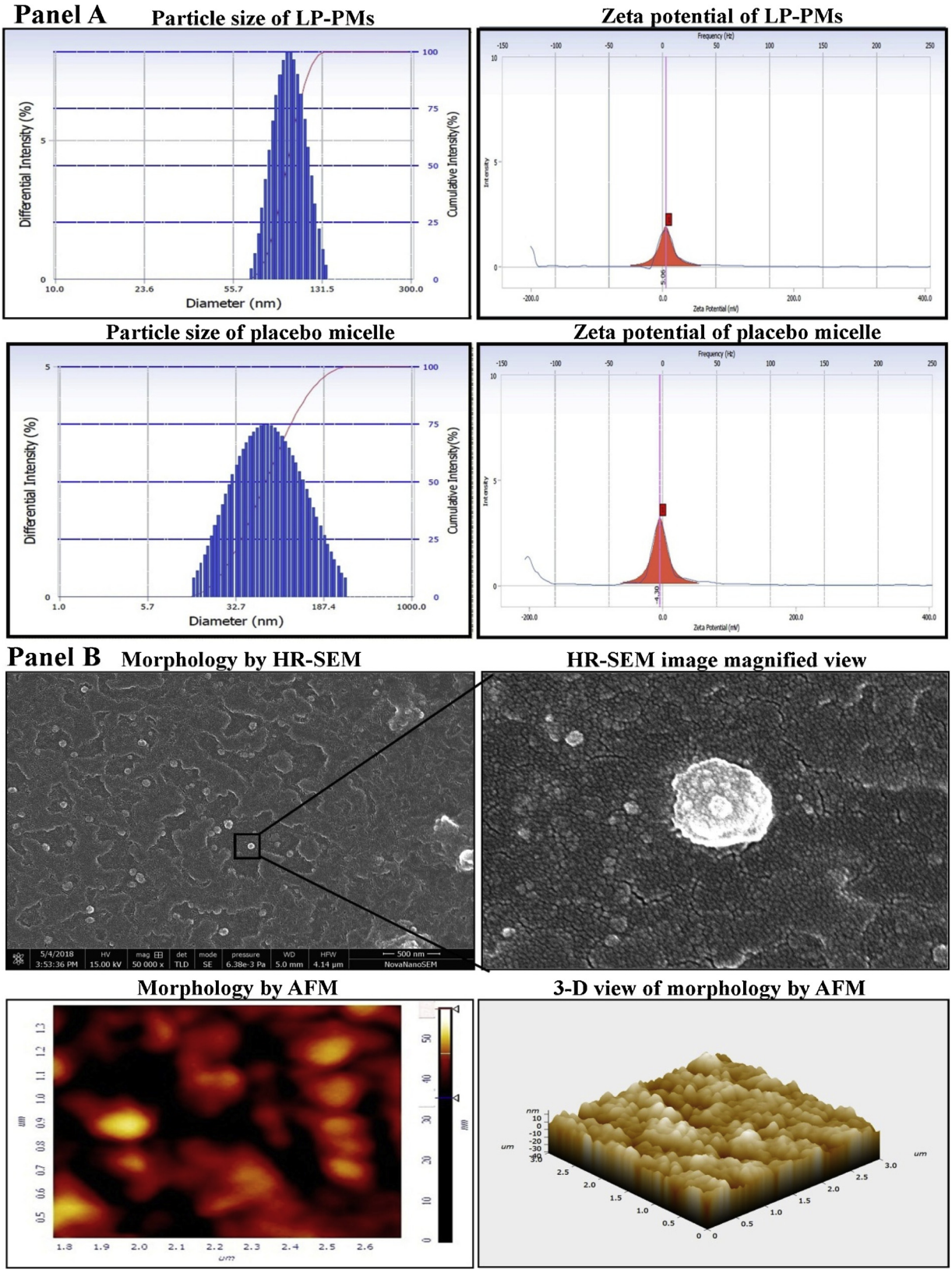

Fig. 3. Morphological characterization of LP-PMs Panel A) Histograms showing particle size and their distribution as well as zeta potential determined by dynamic laser scattering technique; Panel B) High Resolution-Scanning Electron Microscopic images revealing nearly uniform and round shaped morphology and Atomic Force Microscopic images depicting 2-dimensional and 3-dimensional morphology.

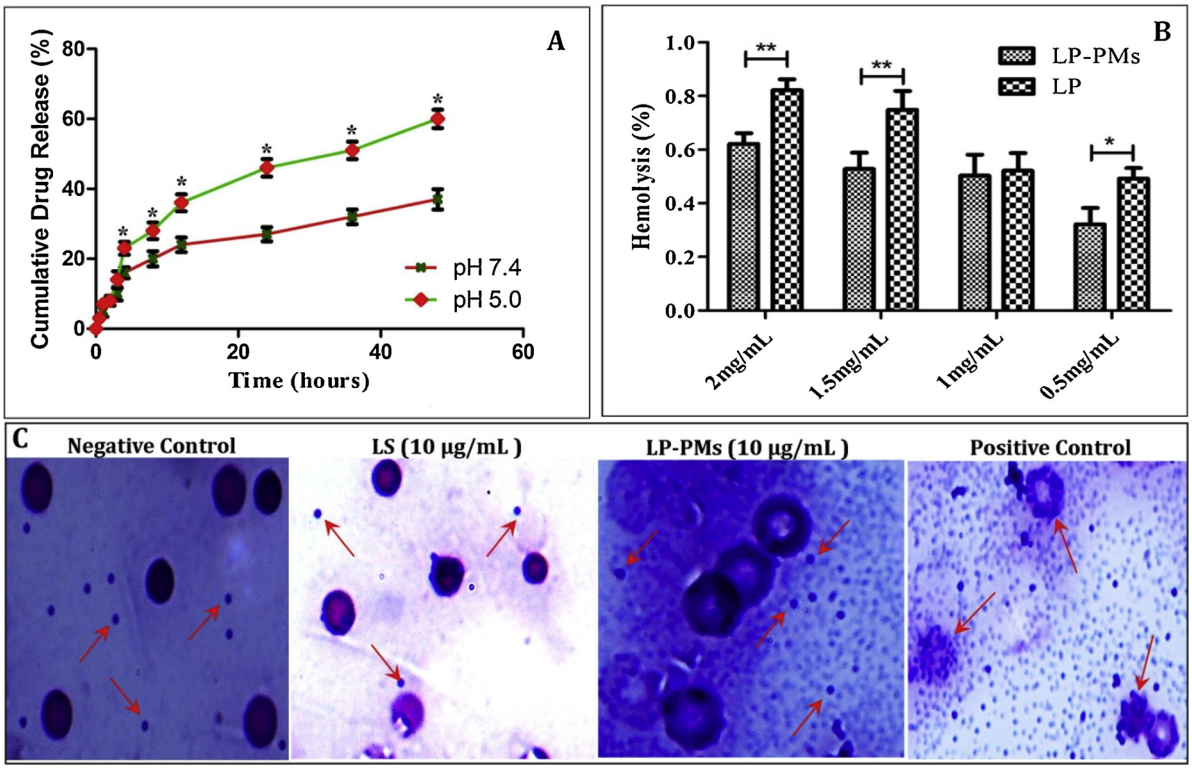

Fig. 4. (A) *In-vitro* drug release profile of Lapatinib-loaded polymeric micelles (LP-PMs) in release media of pH 7.4 and pH 5.0 indicating preferential drug release at lower pH; (B and C) Hemocompatibility testing where (B) represents percent hemolysis caused by different concentrations of LP-PMS and LP only; where * represents significant ($p < 0.05$) difference and **represents significant ($p < 0.01$) difference Shelf life plot for LP-PMs and (C) illustrates no platelet aggregation observed after the treatment of whole blood with retained original morphology of platelets.

the observed initial decrease in the PDI may have been due to the uniform film formation during the solvent evaporation, where the optimum surfactant have reduced the surface tension, resulting in uniform hydration of the thin film and PMs of similar size with a smaller PS distribution. Conversely, high polymer or surfactant contents may have had an impact on the hydration phase, and therefore PMs with wide particle-size ranges were prepared, resulting in high PDI values. Thus, it could be concluded that for the manufacture of nanocolloids (PMs) of uniform size, optimum levels of the polymer as well as the surfactants need to be carefully chosen.

The optimised formulation of the LP-PMs was then characterised in terms of its physicochemical properties. XRPD and FT-IR analyses were performed for solid-state characterization of the optimised formulation. The FT-IR spectra of the physical mixture and the LP-PMs retained peculiar characteristic peaks corresponding to polymers and LP, confirming their compatibility. However, the broadening of the band centred at 3350 cm^{-1} of LP-PMs than other individual spectra may suggest intermolecular hydrogen bonding between the LP and Soluplus® [43,44], which may explain the increased solubility of the drug in the presence of Soluplus®.

Further, the XRPD results implied the successful incorporation of LP within the micelle in the amorphous form. The XRPD profile was rather similar to those of PF127 and Soluplus®, revealing that the outer shell consisted of Soluplus® with a sheath of PF127 over the micelle. Hence, the results confirmed the core–shell structure of micelles incorporating the drug inside the core within the polymeric shell [24].

The lower PDI of the optimised formulation confirmed the successful preparation of monodispersed and uniform-sized micelles. The hydrophilic moieties of PEG-containing −OH functional groups in the molecule of Soluplus® and the free −OH groups of in the molecule of PF127 conveyed a negative zeta potential to blank micelles [45]. However, FT-IR studies confirmed the intermolecular hydrogen bonding between LP and the free −OH groups of Soluplus® and PF127, which might have resulted in the reduction in number of free −OH groups, which contributed to negative zeta potential of blank micelles. Also, LP was reported to partially neutralise the negative charges on the surfaces of micelles [24]. This may be the reason of positive zeta potential observed for LP-PMs.

For better accumulation in the tumour tissue, micelles must be small enough (< 200 nm). Because the size of the prepared LP-PMs was

Table 3
Results of evaluations before and after stability studies.

Conditions	Results of evaluations[a]					
	30 °C ± 2 °C/65% RH ± 5% RH			5 °C ± 3 °C		
Time (month)	PS (nm)	PDI	EE (%)	PS (nm)	PDI	EE (%)
0	92.9 ± 4.07	0.093 ± 0.083	87.23 ± 4.85	92.9 ± 4.07	0.093 ± 0.083	87.23 ± 4.85
3	1041.7 ± 11.32	0.436 ± 0.152	81.11 ± 8.02	94.1 ± 10.42	0.586 ± 0.095	85.04 ± 3.32
6	Discontinued			105.5 ± 12.23	0.635 ± 0.092	82.86 ± 3.94

[a] All the results are mentioned as mean ± standard deviation, n = 3.

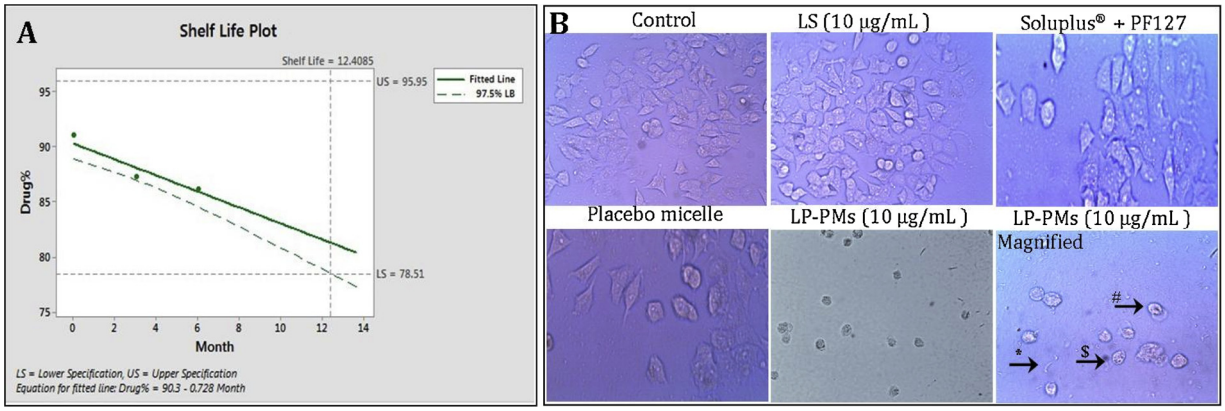

Fig. 5. (A) Shelf-life plot of LP-PMs (B) *In-vitro* anti-cancer efficacy studies of LP-PMs against SKBr3 breast cancer cell line showing apoptosis-like symptoms such as shrinking and round shape of cells due to cytoplasm condensation (arrow with #), nuclear fragmentation (arrow with $) and loss of confluence (arrow with (*), as compared to polygonal and cuboid cells in control group.

below 200 nm, they were thought to have excellent potential for passively targeting tumours by the EPR effect [11].

The EE and DL measure the ability of the selected dosage form to load and deliver the amount of drug to the intended site. The observed high EE was attributed to the increased solubility of LP due to encapsulation in the hydrophobic core of the Soluplus® micelles owing to their core–shell structure. However, free LP forms intermolecular hydrogen bonding with excess Soluplus® (as observed in FT-IR studies) in an aqueous environment. This effect of Soluplus® is responsible for the solubilisation of LP to some extent. Thus, the high encapsulation efficiency of the LP-PMs assures greater drug availability around the target, thereby alleviating the systemic side effects and reducing the required dose of the drug.

In-vitro drug release was performed at two pH conditions to simulate LP-PMs behaviours in blood (pH 7.4) and tumour environments (pH 5.0). A comparatively higher release of LP [Fig. 4(A)] within the first hour may be attributed to the dissolution of a minor amount of LP that might be present in bulk of the LP-PM dispersion. At the earlier hours, no significant difference was observed in LP release; however, a significant difference ($p < 0.001$) in cumulative drug release was witnessed in both media after 4 h, as illustrated in Fig. 4(A). The drug release data were integrated into different kinetic models, and it was found that the LP release followed the Higuchi model.

The release rate of LP from the micelles was found to be higher at pH 5.0 than at pH 7.4; the weakening and distortion of hydrogen bonding between LP and Soluplus® in an acidic environment might have been the reason for enhanced drug release at the lower pH. This behaviour also benefits the dosage form in terms of avoiding unintended and premature drug release in blood circulation, thus minimising dose-related toxicities. Further, the LP-PMs were found to sustained the release of the drug cargo as the micelles rigorously maintained their integrity against dissociation and avoided drug release via small dilutions in the bulk of the body fluids [37,46]. Our findings indicated that nanocolloidal LP-PMs can be employed as sustained release dosage forms for delivery of poorly water-soluble drugs and can successfully and selectively deliver the drug cargo to an acidic tumour environment.

Because LP-PMs were intended for I.V. administration, they must exhibit hemocompatibility. Thus, we investigated and confirmed their hemocompatibility in terms of induced hemolysis *in-vitro* and platelet aggregation after treatment with LP-PMs. Incompatibility with blood components may either cause emboli formation or lead to RBC hemolysis, increasing risk to the patient [47]. Induced hemolysis of < 1% upon I.V. administration is considered safe for patients [48]. Our findings confirmed the hemocompatibility of LP-PMs because significantly lower hemolysis ($p < 0.01$) was found in the LP-PMs than in the LP-only group because of the encapsulation of LP inside the micelle. No aggregation with retained morphology of platelets was observed in the treatment with LP-PMs, indicating its hemocompatibility [47]. Our findings thus establish that micellar encapsulation of LP-rendered LP-PMs offers not only hemolytic protection but also a suitable and safe nanocarrier for I.V. administration.

Stability studies were conducted on LP-PMs to evaluate the effect of environmental conditions on LP-PMs and to recommend suitable conditions for its storage. Based on the PS and EE observations, it was concluded that refrigerated conditions should be recommended for the storage of LP-PMs.

Lastly, it is mandatory to verify whether encapsulation of LP in micellar form could retain its anticancer efficacy. The cytotoxicity and anti-cancer potential of LS and LP-PMs were estimated in terms of morphological changes. LP-PM-treated cells induced apoptosis in SKBr3, which was confirmed by shrinkage and the round morphologies of the cells due to cytoplasmic condensation [49,50], whereas a granular appearance indicated chromatin shrinking or nuclear fragmentation [51]. Our results agree with those of previous studies, as evidenced by the observed change in morphology and the reduced the number of viable cells in the LP-PM treatment group in comparison with the untreated group. The LS group also showed cytotoxicity, but the effect was superseded in the LP-PMs and can be credited to the higher solubilisation or uptake of LP after micellisation. However, mixture of surfactant and placebo micelle without drug did not show toxicity of the SKBr3 cells.

In conclusion, we suggest that Soluplus® micelles can serve as nanocolloidal carriers of LP by the I.V. route without compromising its anti-cancer efficacy. Further studies to evaluate the *in-vivo* performance of the LP-PMs, however, will be required, as we plan.

5. Conclusion

We successfully developed nanocolloidal polymeric micelles for the delivery of the highly hydrophobic drug lapatinib, an anti-cancer agent used for the treatment of breast cancer. The uniform, spherical nanosize (below 150 nm) of these micelles makes them useful for passive tumour targeting by the EPR effect. Soluplus® has a very low CMC, which further decreased by its combination with PF127, which not only provided the system with thermodynamic and kinetic stability but also explained the resistivity of the LP-PMs to dilution in a large pool of body fluids. Hence, it can be successfully employed as a drug carrier for both oral and intravenous administration. *In-vitro* percent cumulative drug release studies demonstrated that the LP-PMs exhibited preferential, enhanced, and sustained drug release at an acidic tumour environment as compared to blood, which indicated the safe transport

of LP in blood. Significantly lower hemolysis in the presence of LP-PMs than of a free LP suspension indicated the safety and potential of LP-PMs for intravenous administration. The cytotoxic effect of LP was retained rather than enhanced by encapsulation as PMs. All these findings establish that the Soluplus® nanocolloidal polymeric micelles can potentially be employed as a successful hydrophobic drug carrier in order to expand clinical applications and improve the effectiveness of lapatinib in breast cancer therapy.

Declaration of Competing Interest

The authors declare that no conflict of interest exists in this article.

Acknowledgements

The authors are grateful for the financial assistance provided by the Ministry of Human Resources and Development, New Delhi (India) and the Department of Pharmaceutical Engineering and Technology, IIT (BHU), Varanasi (U.P., India). Central Instrument Facility Center (CIFC) of IIT (BHU), Varanasi for providing analytical instrumentation facility for various characterizations of LP-PMs. The authors are highly grateful to Mr. Gajanan Awari (BASF India Limited) and BASF India Limited (Navi Mumbai, Maharashtra, India) for kind support by providing gift samples of polymers like Soluplus® and Pluronic® F127.

Appendix A. Supplementary data

Supplementary material related to this article can be found, in the online version, at doi:https://doi.org/10.1016/j.colsurfb.2019.110611.

References

[1] G.V. Bonde, S.K. Yadav, S. Chauhan, et al., Lapatinib nano-delivery systems: a promising future for breast cancer treatment, Expert Opin. Drug Deliv. 15 (5) (2018) 495–507.
[2] F. Ravar, E. Saadat, P.D. Kelishadi, et al., Liposomal formulation for co-delivery of paclitaxel and lapatinib, preparation, characterization and optimization, J. Liposome Res. 26 (3) (2016) 175–187.
[3] E.-G. Jeong, H.J. Yoo, B. Song, et al., Evaluation of lapatinib powder-entrapped biodegradable polymeric microstructures fabricated by X-ray lithography for a targeted and sustained drug delivery system, Materials 8 (2) (2015) 519–534.
[4] H. Zhang, J. Xu, L. Xing, et al., Self-assembled micelles based on chondroitin sulfate/poly (D, L-lactideco-glycolide) block copolymers for doxorubicin delivery, J. Colloid Interface Sci. 492 (2017) 101–111.
[5] D.A. Chiappetta, A. Sosnik, Poly (ethylene oxide)–poly (propylene oxide) block copolymer micelles as drug delivery agents: improved hydrosolubility, stability and bioavailability of drugs, Eur. J. Pharm. Biopharm. 66 (3) (2007) 303–317.
[6] S.J.T. Rezaei, H.S. Abandansari, M.R. Nabid, et al., pH-responsive unimolecular micelles self-assembled from amphiphilic hyperbranched block copolymer for efficient intracellular release of poorly water-soluble anticancer drugs, J. Colloid Interface Sci. 425 (2014) 27–35.
[7] J. Fang, T. Sawa, H. Maeda, Factors and Mechanism of “EPR” Effect and the Enhanced Antitumor Effects of Macromolecular Drugs Including SMANCS, Polymer Drugs in the Clinical Stage: Springer, 2004, pp. 29–49.
[8] K. Yoncheva, P. Calleja, M. Agüeros, et al., Stabilized micelles as delivery vehicles for paclitaxel, Int. J. Pharm. 436 (1–2) (2012) 258–264.
[9] Y. Sun, Y. Li, S. Nan, et al., Synthesis and characterization of pH-sensitive poly (itaconic acid)–poly (ethylene glycol)–folate–poly (l-histidine) micelles for enhancing tumor therapy and tunable drug release, J. Colloid Interface Sci. 458 (2015) 119–129.
[10] S. Jafarzadeh-Holagh, S. Hashemi-Najafabadi, H. Shaki, et al., Self-assembled and pH-sensitive mixed micelles as an intracellular doxorubicin delivery system, J. Colloid Interface Sci. 523 (2018) 179–190.
[11] Z.J. Huo, S.J. Wang, Z.Q. Wang, et al., Novel nanosystem to enhance the antitumor activity of lapatinib in breast cancer treatment: therapeutic efficacy evaluation, Cancer Sci. 106 (10) (2015) 1429–1437.
[12] GLOBOCAN. GLOBOCAN, Cancer Incidence, Mortality and Prevalence Worldwide 2012 [cited 2018 May], Available from: (2012) http://globocan.iarc.fr/old/burden.asp?selection_pop=224900&Text-p=World&selection_cancer=3152&Text-c=Breast&pYear=8&type=0&window=1&submit=%C2%A0Execute.
[13] W. Xia, R.J. Mullin, B.R. Keith, et al., Anti-tumor activity of GW572016: a dual tyrosine kinase inhibitor blocks EGF activation of EGFR/erbB2 and downstream Erk1/2 and AKT pathways, Oncogene 21 (41) (2002) 6255.
[14] H. Gao, Y. Wang, C. Chen, et al., Incorporation of lapatinib into core–shell nanoparticles improves both the solubility and anti-glioma effects of the drug, Int. J. Pharm. 461 (1) (2014) 478–488.
[15] J.-J. Lee, S. Nam, J.-H. Park, et al., Nanocomposites based on Soluplus and Angelica gigas Nakai extract fabricated by an electrohydrodynamic method for oral administration, J. Colloid Interface Sci. 484 (2016) 146–154.
[16] F. Alvarez-Rivera, D. Fernández-Villanueva, A. Concheiro, et al., α-Lipoic acid in soluplus® polymeric nanomicelles for ocular treatment of diabetes-associated corneal diseases, J. Pharm. Sci. 105 (9) (2016) 2855–2863.
[17] M. Hu, J. Zhang, R. Ding, et al., Improved oral bioavailability and therapeutic efficacy of dabigatran etexilate via Soluplus-TPGS binary mixed micelles system, Drug Dev. Ind. Pharm. 43 (4) (2017) 687–697.
[18] H. Yu, D. Xia, Q. Zhu, et al., Supersaturated polymeric micelles for oral cyclosporine A delivery, Eur. J. Pharm. Biopharm. 85 (3) (2013) 1325–1336.
[19] D. Xia, H. Yu, J. Tao, et al., Supersaturated polymeric micelles for oral cyclosporine A delivery: the role of Soluplus–sodium dodecyl sulfate complex, Colloids Surf. B Biointerfaces 141 (2016) 301–310.
[20] Zeng Y-c, S. Li, C. Liu, et al., Soluplus micelles for improving the oral bioavailability of scopoletin and their hypouricemic effect in vivo, Acta Pharmacol. Sin. 38 (3) (2017) 424.
[21] J. Zhao, Y. Xu, C. Wang, et al., Soluplus/TPGS mixed micelles for dioscin delivery in cancer therapy, Drug Dev. Ind. Pharm. 43 (7) (2017) 1197–1204.
[22] S.K. Yadav, G. Khan, M. Bansal, et al., Multiparticulate based thermosensitive intrapocket forming implants for better treatment of bacterial infections in periodontitis, Int. J. Biol. Macromol. 116 (2018) 394–408.
[23] P. Dehghan Kelishady, E. Saadat, F. Ravar, et al., Pluronic F127 polymeric micelles for co-delivery of paclitaxel and lapatinib against metastatic breast cancer: preparation, optimization and in vitro evaluation, Pharm. Dev. Technol. 20 (8) (2015) 1009–1017.
[24] Y. Wei, S. Xu, F. Wang, et al., A novel combined micellar system of lapatinib and Paclitaxel with enhanced antineoplastic effect against human epidermal growth factor receptor-2 positive breast tumor in vitro, J. Pharm. Sci. 104 (1) (2015) 165–177.
[25] S. Mourtas, G.P. Michanetzis, Y.F. Missirlis, et al., Haemolytic activity of liposomes: effect of vesicle size, lipid concentration and polyethylene glycol-lipid or arsonolipid incorporation, J. Biomed. Nanotechnol. 5 (4) (2009) 409–415.
[26] E.A. Bender, M.D. Adorne, L.M. Colomé, et al., Hemocompatibility of poly (ε-caprolactone) lipid-core nanocapsules stabilized with polysorbate 80-lecithin and uncoated or coated with chitosan, Int. J. Pharm. 426 (1-2) (2012) 271–279.
[27] P. Mittal, H. Vrdhan, G. Ajmal, et al., Formulation and characterization of genistein-loaded nanostructured lipid carriers: pharmacokinetic, biodistribution and in vitro cytotoxicity studies, Curr. Drug Deliv. 16 (3) (2019) 215–225.
[28] J. Singh, P. Mittal, G. Vasant Bonde, et al., Design, optimization, characterization and in-vivo evaluation of Quercetin enveloped Soluplus®/P407 micelles in diabetes treatment, Artif. Cells Nanomed. Biotechnol. 46 (sup3) (2018) S546–S555.
[29] L. Di Marzio, C. Marianecci, M. Petrone, et al., Novel pH-sensitive non-ionic surfactant vesicles: comparison between Tween 21 and Tween 20, Colloids Surf. B Biointerfaces 82 (1) (2011) 18–24.
[30] R. Mobasseri, M. Karimi, L. Tian, et al., Hydrophobic lapatinib encapsulated dextran-chitosan nanoparticles using a toxic solvent free method: fabrication, release property & in vitro anti-cancer activity, Mater. Sci. Eng. C 74 (2017) 413–421.
[31] S.-Y. Lin, H.-L. Lin, Y.-T. Chi, et al., Influence of soluplus on solid-state properties and physical stability of indomethacin-saccharin co-crystal formation prepared by air-drying process, J. Pharm. Innov. 11 (2) (2016) 109–119.
[32] T. Al Kayal, D. Panetta, B. Canciani, et al., Evaluation of the effect of a gamma irradiated DBM-pluronic F127 composite on bone regeneration in Wistar rat, PLoS One 10 (4) (2015) e0125110.
[33] R. Trivedi, U.B. Kompella, Nanomicellar formulations for sustained drug delivery: strategies and underlying principles, Nanomedicine 5 (3) (2010) 485–505.
[34] J.J. Sheng, Surfactant–Polymer Flooding. Enhanced Oil Recovery Field Case Studies, Elsevier, 2013, pp. 117–142.
[35] Y. Lu, K. Park, Polymeric micelles and alternative nanonized delivery vehicles for poorly soluble drugs, Int. J. Pharm. 453 (1) (2013) 198–214.
[36] M.A. Muherei, R. Junin, Investigating synergism in critical micelle concentration of anionic-nonionic surfactant mixtures: surface versus interfacial tension techniques, Asian J. Appl. Sci. Eng. 2 (2009) 115–127.
[37] E.V. Batrakova, T.K. Bronich, J.A. Vetro, et al., Polymer Micelles as Drug Carriers. Nanoparticulates as Drug Carriers, World Scientific, 2006, pp. 57–93.
[38] N. Rehman, H. Ullah, S. Alam, et al., Surface and thermodynamic study of micellization of non ionic surfactant/diblock copolymer system as revealed by surface tension and conductivity, J. Mater. Environ. Sci. 8 (2017) 1161–1167.
[39] R. Nagarajan, American oil chemists society and consumer specialty products association …. Editor Polymer-Surfactant Interactions. New Horizons: Detergents for the New Millennium Conference Invited Paper (2001).
[40] R.S. Bhuptani, A.S. Jain, D.T. Makhija, et al., Soluplus based polymeric micelles and mixed micelles of lornoxicam: design, characterization and in vivo efficacy studies in rats, Indian J. Pharm. Educ. Res. 50 (2016) 277–286.
[41] E. Bernabeu, L. Gonzalez, M. Cagel, et al., Novel Soluplus®—TPGS mixed micelles for encapsulation of paclitaxel with enhanced in vitro cytotoxicity on breast and ovarian cancer cell lines, Colloids Surf. B Biointerfaces 140 (2016) 403–411.
[42] C. Oerlemans, W. Bult, M. Bos, et al., Polymeric micelles in anticancer therapy: targeting, imaging and triggered release, Pharm. Res. 27 (12) (2010) 2569–2589.
[43] S. Knop, T.L.C. Jansen, J. Lindner, et al., On the nature of OH-stretching vibrations in hydrogen-bonded chains: pump frequency dependent vibrational lifetime, Phys. Chem. Chem. Phys. 13 (10) (2011) 4641–4650.
[44] T. Yamashita, K. Takatsuka, Hydrogen-bond assisted enormous broadening of infrared spectra of phenol-water cationic cluster: an ab initio mixed quantum-classical study, J. Chem. Phys. 126 (7) (2007) 074304.
[45] X. Jin, B. Zhou, L. Xue, et al., Soluplus® micelles as a potential drug delivery system

for reversal of resistant tumor, Biomed. Pharmacother. 69 (2015) 388–395.
[46] D. Lombardo, M.A. Kiselev, S. Magazù, et al., Amphiphiles self-assembly: basic concepts and future perspectives of supramolecular approaches, Adv. Condens. Matter Phys. 2015 (2015).
[47] P. Mittal, H. Vardhan, G. Ajmal, et al., Formulation, optimization, hemocompatibility and pharmacokinetic evaluation of PLGA nanoparticles containing paclitaxel, Drug Dev. Ind. Pharm. 45 (3) (2019) 365–378.
[48] G. Ajmal, G.V. Bonde, S. Thokala, et al., Ciprofloxacin HCl and quercetin functionalized electrospun nanofiber membrane: fabrication and its evaluation in full thickness wound healing, Artif. Cells Nanomed. Biotechnol. 47 (1) (2019) 228–240.
[49] P. Cancemi, M. Buttacavoli, F. D'Anna, et al., The effects of structural changes on the anti-microbial and anti-proliferative activities of diimidazolium salts, New J. Chem. 41 (9) (2017) 3574–3585.
[50] M. Buttacavoli, N.N. Albanese, G. Di Cara, et al., Anticancer activity of biogenerated silver nanoparticles: an integrated proteomic investigation, Oncotarget 9 (11) (2018) 9685.
[51] G. D'Suze, A. Rosales, V. Salazar, et al., Apoptogenic peptides from Tityus discrepans scorpion venom acting against the SKBR3 breast cancer cell line, Toxicon 56 (8) (2010) 1497–1505.